210 Chem. Mater. **1995,** 7, 210−214

Electronic and Magnetic Properties of Organometallic Intercalates of Zirconium Dichalcogenides

Heng-Vee Wong, Richard Millett, John S. O. Evans, Stephen Barlow, and Dermot O'Hare*

Inorganic Chemistry Laboratory, South Parks Road, Oxford OX1 3QR, UK

Received August 10, 1994. Revised Manuscript Received October 24, 1994⊗

The organometallic sandwich complexes $M(\eta\text{-}C_5H_5)_2$ (M = Co, Cr), $Ti(\eta\text{-}C_5H_5)(\eta\text{-}C_8H_8)$, and $M(\eta\text{-}C_5H_4Me)(\eta\text{-}C_7H_7)$ (M = Mo, W) have been intercalated into the lamellar host lattices ZrS_2, ZrSSe, and $ZrSe_2$. Variable-temperature electrical resistivity measurements have been performed on single-crystal samples of $ZrS_2\{Co(\eta\text{-}C_5H_5)_2\}_{0.25}$, $ZrS_2\{Ti(\eta\text{-}C_5H_5)(\eta\text{-}C_8H_8)\}_{0.2}$, and $ZrS_2\{Cr(\eta\text{-}C_5H_5)_2\}_{0.2}$. The electrical resistivity measurements for $ZrS_2\{(\eta\text{-}C_5H_5)_2\}_{0.25}$ and $ZrS_2\{Ti(\eta\text{-}C_5H_5)(\eta\text{-}C_8H_8)\}_{0.2}$ indicate that they are metallic down to low temperature, exhibiting limiting resistivities of 8.5×10^{-3} and 5.4×10^{-3} Ω cm, respectively, at 4 K. In contrast, $ZrS_2\{Cr(\eta\text{-}C_5H_5)_2\}_{0.2}$ undergoes a metal−semiconductor transition below 25 K. Solid-state magnetic susceptibility measurements have been performed on microcrystalline samples of $ZrS_xSe_{2-x}\{M(\eta\text{-}C_5H_5)_2\}_y$ (M = Co and Cr, x = 0, 1, and 2; y = 0.20−0.22), $ZrS_2\{Ti(\eta\text{-}C_5H_5)(\eta\text{-}C_8H_8)\}_{0.2}$ and $ZrS_2\{M(\eta\text{-}C_5H_4Me)(\eta\text{-}C_7H_7)\}_{0.2}$ (M = Mo and W). The magnetic data for the metallic samples can be fitted to a function comprising a temperature dependent component ($\chi_{\text{Curie−Weiss}}$) and a temperature-independent component (χ_{Pauli}) due to contributions to the molar magnetic susceptibility from the guest ions and conduction electrons respectively. The magnetic susceptibility data suggest that incomplete ionization of the organometallic guests occurs; there appears to be almost no correlation between the electrochemical reduction potential ($E_{1/2}$) and the percentage of guests molecules which are ionized on intercalation.

Introduction

The intercalation of ions and molecules into the layered transition-metal dichalcogenides is a now well-known phenomenon.[1] In almost all cases the reaction is accompanied by electron transfer from the intercalants to the layered host material, where the electron occupies the lowest lying *d* conduction band. Thus, in the case of the group IV dichalcogenides MX_2 (M = Ti, Zr, Hf; X = S, Se) the host lattices are transformed from semiconductors to *d*-band metals upon intercalation. Furthermore, since the conduction bands formed from *d* orbitals on the metal atoms reside in the center of the three-layered MX_2 sandwich, changes in the local bonding are small.

There exists a considerable body of experimental information on the electronic properties of the alkali metal and amine intercalates of transition-metal dichalcogenides; they are found to show the metallic properties expected from the filling of the transition metal *d* band due to electron transfer from the guest to the host.[2] However, relatively little is known about the electronic properties of intercalation compounds formed by insertion of electron-rich organometallic guests such as $M(Cp)_2$ {M = Cr or Co; Cp = $\eta\text{-}C_5H_5$}, Ti(Cp)(COT) {COT = $\eta\text{-}C_8H_8$}, and M(Cp′)(CHT) {M = Mo or W; Cp′ = $\eta\text{-}C_5H_4Me$; CHT = $\eta\text{-}C_7H_7$} into the layered metal dichalcogenides. In addition, while there is little controversy that metallic behavior is often conferred upon metal dichalcogenides upon intercalation of molecular guests, little is known about the degree of charge transfer or the mechanism of the electron scattering in these materials. For example, the electron-pairing mechanism in the 8.3K type II superconductor $SnSe_2\{Co(Cp)_2\}_{0.3}$ is still unknown.[3]

In this paper we describe a systematic study of the electrical and magnetic properties of the intercalation compounds formed by insertion of a range of electron-rich organometallic guests into the semiconducting host lattice ZrS_2.

Experimental Section

Synthesis of Host Lattices. Microcrystalline ZrS_2 was formed by heating stoichiometric quantities of elemental Zr and S, with a 1% molar excess of S, at 900 °C for 1 week in evacuated, sealed silica ampules.[4] Typically 3.864 g of finely divided Zr wire (99.9%, Aldrich) and 2.774 g of S (99.9%, Aldrich) were loaded into a 10 cm (length) × 1.5 cm (internal diameter) ampule. The purple ZrS_2 so formed had a reddish tinge (ZrS_3) and was therefore ground under a nitrogen atmosphere and reannealed at 900 °C for another week to give a free-flowing, purple-black powder. The purity of the ZrS_2 was checked by powder X-ray diffraction. Small quantities of ZrS_3 impurities, if present, were removed by sublimation at 900 °C in an evacuated silica ampule. Single crystals of ZrS_2

⊗ Abstract published in *Advance ACS Abstracts,* December 1, 1994.

(1) (a) Jacobson, A. J. In *Solid State Chemistry: Compounds;* Cheetham, A. K., Day, P., Eds.; Oxford University Press: Oxford, 1992. (b) O'Hare, D. In *Inorganic Materials*; Bruce, D. W., O'Hare, D., Eds.; Wiley: Chichester, 1992. (c) Whittingham, M. S. *Prog. Solid State Chem.* **1978**, *12*, 41. (d) Whittingham, M. S.; Dines, M. B. *Surv. Prog. Chem.* **1980**, *9*, 55.

(2) (a) Liang, W. Y. In *Intercalation in Layered Materials*, Dresselhaus, M. S., Ed.; Plenum Press: New York, 1986; p 31. (b) Friend, R. H.; Yoffe, A. D. *Adv. Phys.* **1987**, *36*, 1.

(3) (a) O'Hare, D.; Wong, H. V.; Hazell, S.; Hodby, J. W. *Adv. Mater.* **1992**, *4*, 658. (b) Formstone, C. A.; Fitzgerald, E. T.; O'Hare, D.; Cox, P. A.; Kurmoo, M.; Hodby, J. W.; Lillicrap, D.; Goss-Custard, M. *J. Chem. Soc., Chem. Commun.* **1990**, *501*.

(4) Balchin, A. A. In *Crystallography and Crystal Chemistry of Materials with Layered Structures;* Levy, F., Ed.; D. Reidel Publishing Company: Dordrecht, Holland, 1976; p 1.

0897-4756/95/2807-0210$09.00/0

were grown by iodine vapor transport; typically ca. 1 g of microcrystalline ZrS_2 was sealed with iodine (4 mg/cm^3 of ampule volume) in an evacuated silica ampule (25 cm × 1.5 cm internal diameter, 10^{-3} Torr) and heated in a three-zone furnace. A linear temperature gradient between 900 and 800 °C was established in the furnace with the ZrS_2 charge sitting in the hot end. The sample was left to transport for a week, after which the ampule was cracked open to yield large platelike crystals of ZrS_2 (ca. 4 mm × 3 mm × 0.2 mm). The crystals, which hydrolyze slowly in moist air, were handled and stored under dry nitrogen. The powder X-ray diffraction patterns of the products corresponded closely with those available from the JCPDS-ICDD database (International Centre for Diffraction Data, Swarthmore, PA 19081).

Synthesis of Organometallic Guests. All solvents used were predried over anhydrous 4 Å zeolite molecular sieves, before distillation under an atmosphere of dinitrogen from Na, K, or Na/K alloy. The solvents were stored under N_2 in Young's ampules containing activated zeolite molecular sieves and were thoroughly degassed before use. The guest molecules $Co(Cp)_2$,[5] $Cr(Cp)_2$,[6] Ti(Cp)(COT),[7] Mo(Cp′)(CHT),[8] and W(Cp′)(CHT)[8] were prepared by established literature methods.

Synthesis of Large Crystal Intercalates. Large single crystals of host were trimmed using a sharp scalpel to ca. 2 mm × 2 mm × 0.2 mm pieces and added to a toluene solution of the desired organometallic species under a nitrogen atmosphere. The reactants were heated to 120 °C, without stirring, for 1 week before washing with several aliquots of toluene and drying in vacuo. The intercalates all showed significant visible expansion along the *c* axis of the crystals. The intercalates were oxygen sensitive and all physical measurements and crystals mounting was carried out under a nitrogen atmosphere. Full intercalation of these crystals was confirmed by elemental microanalysis and by X-ray powder diffraction which showed the absence of any host reflections.

Resistivity Measurements. For electrical resistivity measurements all air-sensitive crystal samples were mounted onto eight-pin dual-in-line (DIL) headers in a glovebox fitted with a stereo zoom optical microscope. Four strips of conducting silver paint (duPont) were applied in bands all around the crystal to enable standard four-point resistivity measurements. This paint configuration ensured that microcracks or interlayer cleavage in the crystals due to mechanical stress did not produce ohmic contacts. The purpose-built apparatus for resistivity measurements was based on modules so that existing commercially available electronics components could be easily interfaced into the system. The rig consists of three modules; the *temperature control*, the *data measurement*, and the *acquisition* systems. Resistance measurements were recorded in either ac or dc mode. All electrical leads were grounded to reduce electrical noise. Typically, for ac measurements, currents of 25 or 100 mA and frequencies of 10 or 33 Hz were passed through the sample, across which the potential drop was measured by a Princeton Lock-In Amplifier Model 5210 interfaced to a Viglen microcomputer running Microsoft Windows compatible software developed in Oxford. Temperature changes of ±1 K/min were employed between 4 and 300 K for both warming and cooling cycles to allow complete temperature equilibration of the sample within the cryostat. For dc measurements, a Hewlett-Packard HP 3478 multimeter, operating in the manual entry mode and IEEE-interfaced to a Viglen microcomputer, was used to obtain four-probe resistance measurements directly. All the resistance data obtained were converted to resistivity units (Ω cm) by measuring the crystal dimensions immediately after the experiment.

Magnetic Susceptibility Measurements. Magnetic susceptibility measurements were obtained between 6 and 300 K on a Cryogenics Consultants SCU 500 SQUID magnetometer in conjunction with a Lakeshore DRC-91C temperature controller. Microcrystalline samples were loaded under nitrogen into either silica or gelatin holders and stoppered with a rubber seal before transferring to the cryostat. All magnetization data were corrected for intrinsic diamagnetic susceptibility of the sample holders and the electronic cores of the constituent atoms.

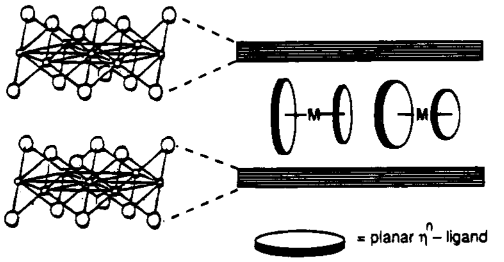

Figure 1. Schematic diagram of the orientational preferences of sandwich complexes intercalated into ZrS_2.

The diamagnetic susceptibilities of the intercalates were obtained by summation of the contributions from the host, obtained form Pascal's constants,[9] and the guests, obtained from Pascal's constants[9] or from the values reported by König et al.[10]

Results and Discussion

Synthesis. The organometallic guest complexes $Co(Cp)_2$ (M = Co, Cr) Ti(Cp)(COT), and M(Cp′)(CHT) (M = Mo and W) can be readily intercalated into the host lattices ZrS_2, ZrSSe, and $ZrSe_2$ by refluxing a toluene solution of the appropriate guest with a suspension of the metal dichalcogenide for 2–3 days at 120 °C. Large crystals (ca. 2.0 × 2.0 × 0.2 mm) of the intercalate phases may be obtained by prolonged reflux (1–2 weeks) in toluene at 120 °C without mechanical stirring. Chemical microanalysis and X-ray powder diffraction experiments show that these crystals are first-stage intercalation compounds with lattice expansions (Δc) in the range 5.3–7.6 Å.[11] We have recently determined the orientational preferences of these organometallic sandwich complexes intercalated in these lamellar ZrX_2 (X = S, Se) lattices.[11] The results indicate that all these organometallic sandwich complexes adopt a well-ordered arrangement in which their preferred orientation is with the metal-to-ring centroid axes lying parallel to the host layer planes (Figure 1). The stoichiometries of the intercalates can be determined by elemental microanalysis. The highest guest occupancies obtained are consistent with two-dimensional close-packing of the guest molecules in the interlamellar region.[11]

Electrical Conductivity Experiments. Figure 2 shows a plot of the temperature dependence of the electrical resistivity of single crystals of the host lattice ZrS_2 grown by the iodine vapor-phase transport technique. The resistivity of the host ZrS_2 rises dramatically at low temperatures, as expected for a semiconductor with a bandgap of 1.7 eV.[12] However, a nonlinear plot of $\ln(\varrho)$ vs $1/T$ was obtained, indicating that the use of iodine during the vapor phase growth of these crystals

---

(5) Wilkinson, G.; Cotton, F. A.; Birmingham, J. M. *J. Inorg. Nucl. Chem.* **1956**, *2*, 95.

(6) Fisher, E. O. *Inorg. Synth.* 6, 132.

(7) Van Oven, H. O.; DeLiete Meijer, H. J. *J. Organomet. Chem.* **1969**, *19*, 373.

(8) Green, M. L. H.; Ng, D. K. P.; Wong, H.-V. *J. Chem. Soc., Dalton Trans.* **1993**, 3213.

(9) Selwood, P. W. *Magnetochemistry;* Interscience: New York, 1956.

(10) König, E.; Schnakig, R.; Kremer, S.; Kanellakopulos, B.; Klenze, R. *Chem. Phys.* **1978**, *27*, 331.

(11) (a) Wong, H.-V.; Evans, J. S. O.; Barlow, S.; O'Hare, D. *J. Chem. Soc., Chem. Commun.* **1993**, 1589. (b) Wong, H.-V.; Evans, J. S. O.; Barlow, S.; Mason, S. J.; O'Hare, D. *Inorg. Chem.*, in press.

(12) Greenaway, D. L.; Nitsche, R. *J. Phys. Chem. Solids* **1965**, *26*, 1445.

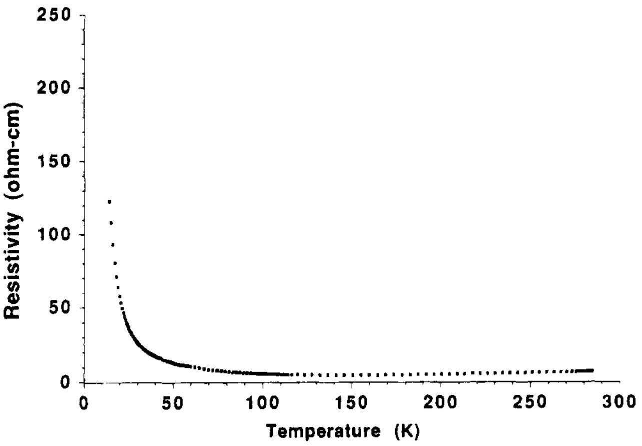

Figure 2. Temperature dependence of the resistivity of single crystals of ZrS_2 in the range 4.2–300 K.

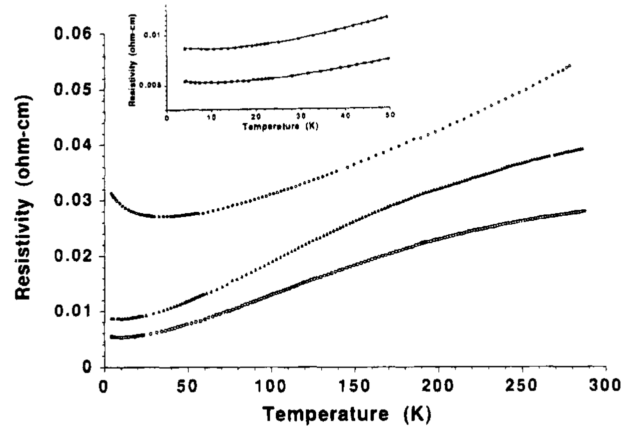

Figure 3. Resistivity of single crystals of the intercalates: (△) $ZrS_2\{Co(\eta\text{-}C_5H_5)_2\}_{0.25}$, (□) $ZrS_2\{Ti(\eta\text{-}C_5H_5)(\eta\text{-}C_8H_8)\}_{0.2}$, and (○) $ZrS_2\{Cr(\eta\text{-}C_5H_5)_2\}_{0.2}$ in the temperature range 4.2–300 K. Inset: Expansion of the low-temperature region for (△) $ZrS_2\{Co(\eta\text{-}C_5H_5)_2\}_{0.25}$ and (□) $ZrS_2\{Ti(\eta\text{-}C_5H_5)(\eta\text{-}C_8H_8)\}_{0.2}$.

had introduced impurities into the band. A plot of $\ln(\varrho)$ vs $(1/T)^{1/3}$ for data below 200 K yielded a straight line characteristic of conduction by two-dimensional variable range hopping.[13,14]

The temperature dependence of the resistivity of the intercalates $ZrS_2\{Co(Cp)_2\}_{0.25}$, $ZrS_2\{Ti(Cp)(COT)\}_{0.2}$, and $ZrS_2\{Cr(Cp)_2\}_{0.2}$ in the temperature range 4.2–300 K is shown in Figure 3. For all the samples metallic behavior was observed down to 30 K. For both $ZrS_2\{Co(Cp)_2\}_{0.25}$ and $ZrS_2\{Ti(Cp)(COT)\}_{0.2}$ the resistivity data behave in accordance with Matthiesen's rule and approach limiting residual resistivities at 4.3 K, ϱ_i, of 8.5×10^{-3} and 5.4×10^{-3} Ω cm for $ZrS_2\{Co(Cp)_2\}_{0.25}$ and $ZrS_2\{Ti(Cp)(COT)\}_{0.2}$, respectively (Figure 3).

For $ZrS_2\{Cr(Cp)_2\}_{0.2}$, on the other hand, localization of electrons occurs below 30 K, and we observe an upturn in the resistivity, suggesting a metal to nonmetal transition. The temperature dependence of $\ln(\varrho)$ below 30 K can be fitted to either a $T^{-1/3}$ or $T^{-1/4}$ dependence. Both plots give reasonably good fits to a straight line, but the fit is marginally better for the latter. The correspondence of resistivity to a $T^{-1/n}$ law ($3 < n < 4$) is good evidence for variable range hopping in this intercalate. Based on the slightly better agreement with the $T^{-1/4}$ law, the hopping is tentatively assigned as a three-dimensional process. The dimensionality of the hopping observed here contrasts with that reported by Sarma[15] for the hydrazine intercalates of 1T-TaS_2 (where $\ln(\varrho) \propto T^{-1/3}$) but is consistent with that in organometallic intercalates such as $SnSe_xS_{2-x}\{Co(Cp)_2\}_{0.3}$ $\{0 \le x \le 2\}$ where three-dimensional variable range hopping was observed.[16]

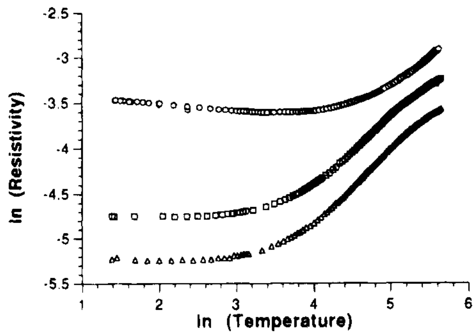

Figure 4. $\ln(\varrho)$ vs $\ln(T)$ for single crystals of the intercalates: (△) $ZrS_2\{Co(\eta\text{-}C_5H_5)_2\}_{0.25}$, (□) $ZrS_2\{Ti(\eta\text{-}C_5H_5)(\eta\text{-}C_8H_8)\}_{0.2}$, and (○) $ZrS_2\{Cr(\eta\text{-}C_5H_5)_2\}_{0.2}$ in the temperature range 4.2–300 K.

The temperature dependence of the resistivity of the intercalates above 30 K is extremely complex. Although the overall trend is that of a metallic character, we have been unable to fit the data to the classical models such as electron–phonon scattering ($\varrho \propto T$), Landau–Baber electron–electron scattering, or combinations of longitudinal acoustic phonons and optical phonons ($\varrho \propto T^2$). In fact a plot of $\ln(\varrho)$ versus $\ln(T)$ (Figure 4) for the three intercalates is nonlinear above 30 K, and no regions show either a T^2 or T^1 dependence.

Magnetic Susceptibility Measurements. In addition to affecting the resistivity of the host, the electron transfer that occurs from the electron-rich guests to the host upon intercalation also manifests itself in significant changes in the temperature dependence of the magnetic susceptibility of the intercalated phase. Magnetic susceptibility experiments can yield important insights into the electronic structure of the host on reduction and, for metallic samples, the magnitude of the weakly temperature-independent Pauli susceptibility (χ_P) can be related to the density of states at the Fermi energy $\{N(E_f)\}$ $\{$where $\chi_P = \mu_B{}^2N(E_f)\}$.

The molar magnetic susceptibility (χ_{total}) has been measured for microcrystalline samples of $ZrS_xSe_{2-x}\{M(\eta\text{-}C_5H_5)_2\}_y$ (M = Co and Cr, x = 0, 1, and 2; y = 0.20–0.22), $ZrS_2\{Ti(\eta\text{-}C_5H_5)(\eta\text{-}C_8H_8)\}_{0.2}$, and $ZrS_2\{M(\eta\text{-}C_5H_4Me)(\eta\text{-}C_7H_7)\}_{0.2}$ (M = Mo and W) in the temperature range 6–300 K. After correction for the intrinsic diamagnetism of the core electrons of the constituent atoms, χ_d, we have fitted the magnetic susceptibility data to eq 1 and Tables 1 and 2 summarize the χ_d, χ_P,

$$\chi_{Total} = \chi_{Pauli} + \chi_{Curie-Weiss} \qquad (1)$$

μ_{eff}, and θ values obtained for all the intercalate

---

[13] Mott, N. F.; Davis, E. A. *Electronic Processes in Non-Crystalline Materials*; Clarendon Press: Oxford, 1971.

[14] (a) Klipstein, P. C.; Bagnall, A. G.; Liang, W. Y.; Marseglia, E. A.; Friend, R. H. *J. Phys. C* **1981**, *14*, 4067. (b) Ghorayeb, A. M.; Friend, R. H. *J. Phys. C* **1987**, *20*, 4181. (c) Ahmad, N.; Klipstein, P. C.; Obertelli, S. D., Marseglia, E. A.; Friend, R. H. *J. Phys. C: Solid State Phys.* **1987**, *20*, 4105.

[15] Sarma, M.; Beal, A. R.; Nulsen, S.; Friend, R. H. *J. Phys. C* **1982**, *15*, 477.

[16] Formstone, C. A.; Kurmoo, M.; Fitzgerald, E. T.; Cox, P. A.; O'Hare, D. *J. Mater. Chem.* **1991**, *1*, 51.

Table 1. Magnetic Susceptibilities, Diamagnetic and Pauli, for $ZrS_xSe_{2-x}\{M(\eta\text{-}C_5H_5)_2\}_y$ {M = Co, Cr; x = 0, 1, or 2; y = 0.2–0.22}, $ZrS_2\{Ti(\eta\text{-}C_5H_5)(\eta\text{-}C_8H_8)\}_{0.2}$, $ZrS_2\{Mo(\eta\text{-}C_5H_4Me)(\eta\text{-}C_7H_7)\}_{0.2}$, and $ZrS_2\{W(\eta\text{-}C_5H_4Me)(\eta\text{-}C_7H_7)\}_{0.2}$

compound	χ_d (10^{-6} emu mol^{-1})	χ_p (10^{-6} emu mol^{-1})
$ZrS_2\{Co(Cp)_2\}_{0.25}$	−123	195
$ZrSSe\{Co(Cp)_2\}_{0.22}$	−133	83
$ZrSe_2\{Co(Cp)_2\}_{0.22}$	−144	180
$ZrS_2\{Cr(Cp)_2\}_{0.2}$	−91	370
$ZrSSe\{Cr(Cp)_2\}_{0.2}$	−100	200
$ZrSe_2\{Cr(Cp)_2\}_{0.2}$	−110	150
$ZrS_2\{Ti(Cp)(COT)\}_{0.2}$	−94	20
$ZrS_2\{Mo(Cp')(CHT)\}_{0.2}$	−97	75
$ZrS_2\{W(Cp')(CHT)\}_{0.2}$	−99	175

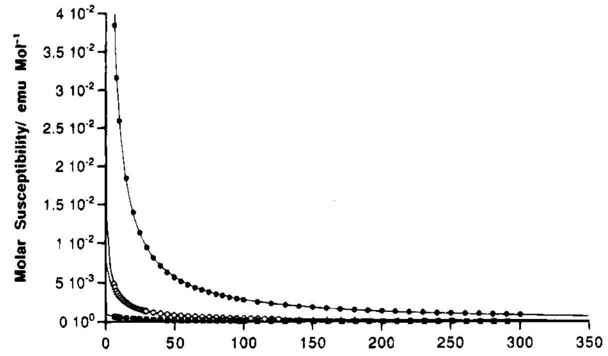

Figure 5. Temperature dependence on the molar magnetic susceptibility (χ_M) for (■) $ZrS_2\{Co(\eta\text{-}C_5H_5)_2\}_{0.25}$, (○) $ZrS_2\{Mo(\eta\text{-}C_5H_4Me)(\eta\text{-}C_7H_7)\}_{0.2}$, (+) $ZrS_2\{W(\eta\text{-}C_5H_4Me)(\eta\text{-}C_7H_7)\}_{0.2}$, and (●) $ZrS_2\{Cr(\eta\text{-}C_5H_5)_2\}_{0.2}$ in the range 4.2–300 K. The solid lines are lest squares fits to eq 1.

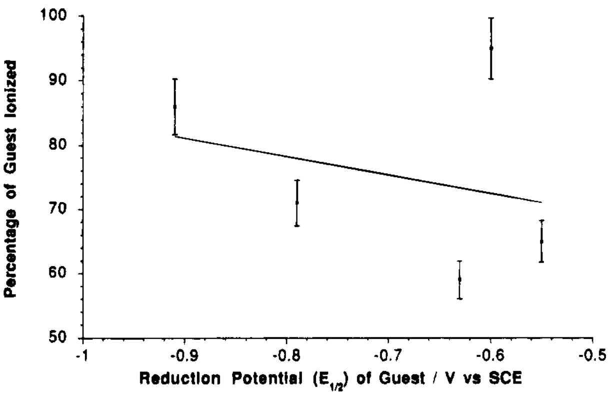

Figure 6. Plot of the degree of guest ionization vs guest electrochemical redox potential ($E_{1/2}$) for the organometallic intercalates of ZrS_2.

samples. In eq 1 χ_{Pauli} is the weak temperature independent paramagnetism associated with metallic electrons and $\chi_{\text{Curie-Weiss}}$ is the temperature-dependent paramagnetism due to localized electrons.

All the intercalate phases show some degree of Curie–Weiss paramagnetism. Figure 5 shows a plot of χ_{total} versus T for several of the intercalates. Since, magnetic susceptibility measurements by Ahmad on $LiZrS_2$ have shown that it exhibits temperature-independent Pauli paramagnetism, and no Curie paramagnetism from localized electrons in ZrS_2 we have assumed a similar behavior for the electron donated to the ZrS_2 lattice by the organometallic complexes. Thus the effective magnetic moment of the intercalates $\{\mu_{\text{eff}}^2(\text{intercalate})\}$ is given by eq 2, where z is the total chemical occupancy

$$\mu_{\text{eff}}^2(\text{intercalate}) = (z - x)\mu_{\text{eff}}^2(\text{guest}) + x\mu_{\text{eff}}^2(\text{guest}^+) \qquad (2)$$

of the guest molecules and x is the occupancy of ionized guest molecules Therefore, we can estimate the degree of electron transfer from the guest molecules to the ZrS_2 host lattice ($x/z \times 100$)% knowing the total chemical occupancy (z) and the effective magnetic moment $\{\mu_{\text{eff}}(\text{intercalate})\}$. The measured magnetic moment data are tabulated in Table 2 and compared with two conventional measures of the ease of ionization of these organometallics; the gas-phase ionization potential (IP) and the electrochemical reduction potential (E^+/E°).

The results indicate the calculated percentage of ionized guest molecules is critically dependent on the accuracy of the molecular stoichiometry obtained from the elemental microanalytical data. For example, if we assume that intercalate stoichiometries are $ZrS_2\{G\}_{0.2\pm0.02}$ then we have an uncertanity of ±10% in the percentages of guest ionized. Nevertheless, the magnetic susceptibility data suggest that in many cases incomplete ionization of the organometallic guests occurs. However, there appears to be no obvious correlation between the extent of ionization and the electrochemical oxidation potential of the guest (Figure 6).

For metallic intercalation compounds large temperature-independent Pauli susceptibilities have been mea-

Table 2. Measured Effective Magnetic Moments (μ_{eff}) and Weiss Constants (θ) for the Organometallic Intercalates of Zirconium Dichalcogenides

	obsd						
compound	$\mu_{\text{eff}}/(\mu_B)$,	θ/(deg)	calcd $\mu_{\text{eff}}^{G}/(\mu_B)^c$	calcd $\mu_{\text{eff}}^{G+}/(\mu_B)^d$	% of guests ionized[a]	guest IP/(eV)	guest $E^+/E^\circ/(V)^b$
$ZrS_2\{Co(Cp)_2\}_{0.25}$	0.32(3)	−8.5(8)	0.87	0	86	5.56[19]	−0.91[20]
$ZrSSe\{Co(Cp)_2\}_{0.29}$	0.38(4)	−14.8(14)	0.93	0	84	5.56	−0.91
$ZrSe_2\{Co(Cp)_2\}_{0.29}$	0.25(2)	−1.6(1)	0.93	0	93	5.56	−0.91
$ZrS_2\{Cr(Cp)_2\}_{0.20}$	1.58(15)	−1.7(1)	1.35	1.73	57	5.70[19]	−0.55[21]
$ZrSSe\{Cr(Cp)_2\}_{0.2}$	1.52(15)	−1.5(1)	1.35	1.73	42	5.70	−0.55
$ZrSe_2\{Cr(Cp)_2\}_{0.2}$	1.43(14)	−1.6(1)	1.35	1.73	19	5.70	−0.55
$ZrS_2\{W(Cp')(CHT)\}_{0.2}$	0.65(6)	−6.5(6)	0	0.77	71	5.50[22]	−0.79[8]
$ZrS_2\{Mo(Cp')(CHT)\}_{0.2}$	0.59(6)	−2.8(3)	0	0.77	59	5.70[23e]	−0.63[8]
$ZrS_2\{Ti(Cp)(COT)\}_{0.2}$	0.09(1)	2.6(2)	0.77	0	98	5.67[24]	−0.60[25]
$SnSe_2\{Co(Cp)_2\}_{0.3}$	0.24(2)	−1.5(1)	0.94	0	94	5.56	−0.91
$SnS_2\{Co(Cp)_2\}_{0.3}$	0.36(4)	−13.7(13)	0.94	0	86	5.56	−0.91

[a] Percentage of fully ionized organometallic guest is calculated by ($x/z \times 100$)% using eq 2. [b] Half-wave potentials ($E_{1/2}$/V vs SCE) for the guest$^+$/guest° reduction. [c] Effective moment assuming all the intercalated guest molecules remain un-ionized. [d] Effective moment assuming all the intercalated guest molecules are singly ionized. Calculated effective moments based on $\mu_{\text{eff}}\{Co(Cp)_2\} = 1.74\ \mu_B$.[10] $\mu_{\text{eff}}\{Cr(Cp)_2\} = 3.02\ \mu_B$;[10] $\mu_{\text{eff}}\{Cr(Cp)_2^+\} = 3.87\ \mu_B$.[26] $\mu_{\text{eff}}\{M(Cp')(CHT)^+\} = 1.73\ \mu_B$ (M = Mo, W). $\mu_{\text{eff}}\{Ti(Cp)(COT)\} = 1.71\ \mu_B$.[27] [e] Data for Mo(Cp)(CHT).

sured previously. For example, Murphy et al.[17] have shown that in various lithium intercalates of metal dichalcogenides temperature independent susceptibilities ranging from 10^{-3} to 10^{-5} emu mol^{-1} are observed. Similar measurements by Guy et al.[18] for $TiSe_2(N_2H_4)_{0.6}$ yielded a Pauli susceptibility of 74 × 10^{-6} mol^{-1}, while Ahmad[15] found an increase of 78 × 10^{-6} emu mol^{-1} for the lithium intercalate of ZrS_2 relative to the pristine host.

Both $ZrS_2\{Co(Cp)_2\}_{0.25}$ and $ZrS_2\{Cr(Cp)_2\}_{0.2}$ show significant Pauli susceptibilities of 1.95×10^{-4} and 3.70×10^{-4} emu mol^{-1}, respectively. These values are similar to those reported by Murphy[16] for $LiTiSe_2$ and $LiTiS_2$ (1.77×10^{-4} and 2.46×10^{-4} emu mol^{-1}, respectively). In the absence of detailed information relating to the band structure of these materials and due to the difficulty in assigning formal oxidations to the metal atoms, it is impossible to infer the extent, if any, of Pauli enhancement in these organometallic intercalates.

Conclusions

The electrical resistivities and magnetic susceptibilities of a range of organometallic intercalates of zirconium dichalcogenides have been measured between 4.2 and 300 K. The donation of electrons from the organometallic species to the host material causes these compounds to exhibit metallic behavior down to very low temperatures. The magnetic susceptibility data suggest that in all cases incomplete ionization of the organometallic guests occurs. However, there appears to be no obvious correlation between the percentage ionization for a given lattice and the electrochemical potential of the guest. Both the resistivity and magnetic data indicate that $ZrS_2\{Cr(Cp)_2\}_{0.2}$ is electronically quite different from $ZrS_2\{Co(Cp)_2\}_{0.25}$ and $ZrS_2\{Ti(Cp)(COT)\}_{0.2}$. At low temperatures, localization of electrons occurs within the former but not the latter two compounds. Moreover, the Pauli susceptibility in the chromocene intercalate is also significantly higher than that for the cobaltocene and Ti(Cp)(COT) intercalates. The resistivity and magnetic data are therefore consistent with a narrower band width for $ZrS_2\{Cr(Cp)_2\}_{0.2}$ than the analogous $Co(Cp)_2$ and Ti(Cp)(COT) intercalates.

Acknowledgment. We would like to thank the SERC for financial support and the Rhodes Trust for a scholarship (H.-V.W.).

CM940383Y

---

(17) Murphy, D. W.; DiSalvo, F. J.; Hull, G. W.; Wasczczak, J. W. *Inorg. Chem.* **1976**, *15*, 17.

(18) (a) Guy, D. R. P.; Friend, R. H.; Johnson, D. C.; Sienko, M. J. *J. Phys. C* **1982**, *15*, 1251. (b) Guy, D. R. P.; Friend, R. H.; Harrison, M. R.; Johnson, D. C.; Sienko, M. J. *J. Phys. C* **1982**, *15*, 1245.

(19) Cauletti, C.; Green, J. C.; Kelly, R.; Powell, P.; J. V. T., Robbins, J.; Smart, J. *J. Electron Spectrosc. Relat. Phenom.* **1980**, *19*, 327.

(20) Koelle, U.; Khouzami, F. *Angew. Chem., Int. Ed. Engl.* **1980**, *19*, 640.

(21) Pinsky, B. L. Cited as personal communication in Robbins, J. L.; Edelstein, N.; Spencer, B.; Smart, J. C. *J. Am. Chem. Soc.* **1982**, *104*, 1882.

(22) Ng, D. K. P. D. Philosophy Thesis, University of Oxford, 1993.

(23) Green, J. C.; Kaltsoyannis, N.; Sza, K. H.; MacDonald, M. *J. Am. Chem. Soc.* **1994**, *116*, 1994.

(24) Evans, S.; Green, J. C.; Jackson, S. E.; Higginson, B. *J. Chem. Soc., Dalton Trans.* **1974**, 304.

(25) Anderson, J. E.; Maher, E. T.; Kool, L. B. *Organometallics* **1991**, *10*, 1248.

(26) Fischer, E. O.; Ulm, K. *Chem. Ber.* **1962**, *95*, 692.

(27) Thomas, J. L.; Hayes, R. G. *Inorg. Chem.* **1972**, *11*, 348.